Biomedical Optics EXPRESS

Biochemical characterization of human gingival crevicular fluid during orthodontic tooth movement using Raman spectroscopy

Gyeong Bok Jung,[1,4] Kyung-A Kim,[3,4] Ihn Han,[1] Young-Guk Park,[3,5] and Hun-Kuk Park[1,2,*]

[1]*Department of Biomedical Engineering & Healthcare Industry Research Institute, College of Medicine, Kyung Hee University, 1 Hoegi-dong, Dongdaemun-gu, Seoul 130-701, South Korea*
[2]*Program of Medical Engineering, Kyung Hee University, Seoul 130-701, South Korea*
[3]*Department of Orthodontics, School of Dentistry, Kyung Hee University, 130-701, South Korea*
[4] *These authors contributed equally to this work.*
[5]*ygpark@khu.ac.kr*
[*]*sigmoidus@khu.ac.kr*

Abstract: This study used Raman spectroscopy to report the first human gingival crevicular fluid (GCF) biochemical characterization during the early phase of orthodontic tooth movement. This technique allows for label-free and noninvasive biochemical change monitoring in GCF during orthodontic tooth movement. Ten orthodontic patients (20.8 ± 2.5 years) participated in the study. GCF samples were obtained before (baseline, 0 days) and during orthodontic treatment at 1, 7 and 28 days. For Raman spectroscopic measurement, GCF samples (5 µl) were deposited onto a gold-coated substrate, then dried at room temperature. Raman spectra GCF analysis during orthodontic treatment indicated that the hydroxyapatite to primarily collagen-dominated matrix band (phosphate 984 cm^{-1}/amide I 1667 cm^{-1}) intensity ratio decreased at day 7 ($P < 0.05$). The carbonate apatite to hydroxyapatite ratio (carbonate 1088 cm^{-1}/phosphate 984 cm^{-1}) was significantly higher on day 7 compared to day 0 ($P < 0.05$). These results indicate that demineralization occurs during the alveolar bone remodeling process. We also found notable peak shifts in the amide I range during orthodontic tooth movement. The 1658 cm^{-1} in baseline red shifted to 1667 cm^{-1} at orthodontic treatment day 7. Curve fitting in the amide I (1615-1725 cm^{-1}) range demonstrated that increased random coil conformation was accompanied by a decrease in β-sheet structure during orthodontic tooth movement. Thus, we suggest Raman spectroscopy could be used for label-free, non-invasive GCF quality assessment during orthodontic tooth movement. Furthermore, this method may prove to be a powerful diagnostic and prognostic tool for monitoring orthodontic tooth movement in a clinical setting.

OCIS codes: (170.5660) Raman Spectroscopy; (170.0170) Medical optics and biotechnology; (170.1850) Dentistry (Medical optics and biotechnology); (170.1610) Clinical applications (Medical optics and biotechnology).

References and links

1. P. J. Brooks, D. Nilforoushan, M. F. Manolson, C. A. Simmons, and S. G. Gong, "Molecular markers of early orthodontic tooth movement," Angle Orthod. **79**(6), 1108–1113 (2009).
2. F. d'Apuzzo, S. Cappabianca, D. Ciavarella, A. Monsurrò, A. Silvestrini-Biavati, and L. Perillo, "Biomarkers of periodontal tissue remodeling during orthodontic tooth movement in mice and men: overview and clinical relevance," ScientificWorld J. **2013**, 105873 (2013).
3. Z. Davidovitch, O. F. Nicolay, P. W. Ngan, and J. L. Shanfeld, "Neurotransmitters, cytokines, and the control of alveolar bone remodeling in orthodontics," Dent. Clin. North Am. **32**(3), 411–435 (1988).
4. S. Uematsu, M. Mogi, and T. Deguchi, "Interleukin (IL)-1 beta, IL-6, tumor necrosis factor-alpha, epidermal

#216711 - $15.00 USD Received 9 Jul 2014; revised 28 Aug 2014; accepted 1 Sep 2014; published 10 Sep 2014

growth factor, and beta 2-microglobulin levels are elevated in gingival crevicular fluid during human orthodontic tooth movement," J. Dent. Res. **75**(1), 562–567 (1996).
5. J. M. Goodson, "Gingival crevice fluid flow," Periodontol. 2000 **31**(1), 43–54 (2003).
6. M. C. Alfano, "The origin of gingival fluid," J. Theor. Biol. **47**(1), 127–136 (1974).
7. G. Y. Teng and E. J. Liou, "Interdental osteotomies induce regional acceleratory phenomenon and accelerate orthodontic tooth movement," J. Oral Maxillofac. Surg. **72**(1), 19–29 (2014).
8. A. Dudic, S. Kiliaridis, A. Mombelli, and C. Giannopoulou, "Composition changes in gingival crevicular fluid during orthodontic tooth movement: comparisons between tension and compression sides," Eur. J. Oral Sci. **114**(5), 416–422 (2006).
9. G. Barbieri, P. Solano, J. A. Alarcón, R. Vernal, J. Rios-Lugo, M. Sanz, and C. Martín, "Biochemical markers of bone metabolism in gingival crevicular fluid during early orthodontic tooth movement," Angle Orthod. **83**(1), 63–69 (2013).
10. W. J. Rody, Jr., M. Wijegunasinghe, W. A. Wiltshire, and B. Dufault, "Differences in the gingival crevicular fluid composition between adults and adolescents undergoing orthodontic treatment," Angle Orthod. **84**(1), 120–126 (2014).
11. N. Buduneli, E. Buduneli, E. O. Cetin, L. Kirilmaz, and N. Kütükçüler, "Clinical findings and gingival crevicular fluid prostaglandin E2 and interleukin-1-beta levels following initial periodontal treatment and short-term meloxicam administration," Expert Opin. Pharmacother. **11**(11), 1805–1812 (2010).
12. G. Perinetti, M. Paolantonio, M. D'Attilio, D. D'Archivio, D. Tripodi, B. Femminella, F. Festa, and G. Spoto, "Alkaline phosphatase activity in gingival crevicular fluid during human orthodontic tooth movement," Am. J. Orthod. Dentofacial Orthop. **122**(5), 548–556 (2002).
13. M. Grant, J. Wilson, P. Rock, and I. Chapple, "Induction of cytokines, MMP9, TIMPs, RANKL and OPG during orthodontic tooth movement," Eur. J. Orthod. **35**(5), 644–651 (2013).
14. X. M. Xiang, K. Z. Liu, A. Man, E. Ghiabi, A. Cholakis, and D. A. Scott, "Periodontitis-specific molecular signatures in gingival crevicular fluid," J. Periodontal Res. **45**(3), 345–352 (2010).
15. X. Xiang, P. M. Duarte, J. A. Lima, V. R. Santos, T. D. Gonçalves, T. S. Miranda, and K. Z. Liu, "Diabetes-associated periodontitis molecular features in infrared spectra of gingival crevicular fluid," J. Periodontol. **84**(12), 1792–1800 (2013).
16. S. Feng, R. Chen, J. Lin, J. Pan, Y. Wu, Y. Li, J. Chen, and H. Zeng, "Gastric cancer detection based on blood plasma surface-enhanced Raman spectroscopy excited by polarized laser light," Biosens. Bioelectron. **26**(7), 3167–3174 (2011).
17. I. Barman, N. C. Dingari, A. Saha, S. McGee, L. H. Galindo, W. Liu, D. Plecha, N. Klein, R. R. Dasari, and M. Fitzmaurice, "Application of Raman spectroscopy to identify microcalcifications and underlying breast lesions at stereotactic core needle biopsy," Cancer Res. **73**(11), 3206–3215 (2013).
18. J. Horsnell, P. Stonelake, J. Christie-Brown, G. Shetty, J. Hutchings, C. Kendall, and N. Stone, "Raman spectroscopy- a new method for the intra-operative assessment of axillary lymph nodes," Analyst (Lond.) **135**(12), 3042–3047 (2010).
19. J. Lin, R. Chen, S. Feng, J. Pan, B. Li, G. Chen, S. Lin, C. Li, L. Sun, and Z. Huang, "Surface-enhanced Raman scattering spectroscopy for potential noninvasive nasopharyngeal cancer detection," J. Raman Spectrosc. **43**(4), 497–502 (2012).
20. K. Guze, H. C. Pawluk, M. Short, H. Zeng, J. Lorch, C. Norris, and S. Sonis, "Pilot study: Raman spectroscopy in differentiating premalignant and malignant oral lesions from normal mucosa and benign lesions in humans," Head Neck n/a (2014), doi:10.1002/hed.23629.
21. A. Sahu, S. Sawant, H. Mamgain, and C. M. Krishna, "Raman spectroscopy of serum: an exploratory study for detection of oral cancers," Analyst (Lond.) **138**(14), 4161–4174 (2013).
22. S. Yang, B. Li, A. Akkus, O. Akkus, and L. Lang, "Wide-field Raman imaging of dental lesions," Analyst (Lond.) **139**(12), 3107–3114 (2014).
23. M. Toledano, I. Cabello, M. A. Vílchez, M. A. Fernández, and R. Osorio, "Surface microanalysis and chemical imaging of early dentin remineralization," Microsc. Microanal. **20**(1), 245–256 (2014).
24. G. S. Griffiths, A. M. Moulson, A. Petrie, and I. T. James, "Evaluation of osteocalcin and Pyridinium crosslinks of bone collagen as markers of bone turnover in gingival crevicular fluid during different stages of orthodontic treatment," J. Clin. Periodontol. **25**(6), 492–498 (1998).
25. J. D. Gelder, K. D. Gussem, P. Vandenabeele, and L. Moens, "Reference database of Raman spectra of biological molecules," J. Raman Spectrosc. **38**(9), 1133–1147 (2007).
26. Q. Matthews, A. Jirasek, J. Lum, X. Duan, and A. G. Brolo, "Variability in Raman spectra of single human tumor cells cultured in vitro: correlation with cell cycle and culture confluency," Appl. Spectrosc. **64**(8), 871–887 (2010).
27. J. W. Chan, D. S. Taylor, T. Zwerdling, S. M. Lane, K. Ihara, and T. Huser, "Micro-Raman spectroscopy detects individual neoplastic and normal hematopoietic cells," Biophys. J. **90**(2), 648–656 (2006).
28. R. L. Frost and S. J. Palmer, "A vibrational spectroscopic study of the mixed anion mineral sanjuanite $Al_2(PO_4)(SO_4)(OH)\cdot 9H_2O$," Spectrochim. Acta A Mol. Biomol. Spectrosc. **79**(5), 1210–1214 (2011).
29. J. Urmos, S. K. Sharma, and F. T. Mackenzie, "Characterization of some biogenic carbonates with Raman spectroscopy," Am. Mineral. **76**, 641–646 (1991).
30. S. Mathew, "Orthodontic tooth movement and changes in gingival crevicular fluid: A Review," J. Indian Orthod. Soc. **37**, 101–114 (2004).
31. N. Pender, B. H. A. Samuels, and K. S. Last, "The monitoring of orthodontic tooth movement over a 2-year period by analysis of gingival crevicular fluid," Eur. J. Orthod. **16**(6), 511–520 (1994).
32. A. Carden and M. D. Morris, "Application of vibrational spectroscopy to the study of mineralized tissues

#216711 - $15.00 USD Received 9 Jul 2014; revised 28 Aug 2014; accepted 1 Sep 2014; published 10 Sep 2014

(review)," J. Biomed. Opt. **5**(3), 259–268 (2000).
33. B. R. McCreadie, M. D. Morris, T. C. Chen, D. Sudhaker Rao, W. F. Finney, E. Widjaja, and S. A. Goldstein, "Bone tissue compositional differences in women with and without osteoporotic fracture," Bone **39**(6), 1190–1195 (2006).
34. D. B. Burr, M. R. Forwood, D. P. Fyhrie, R. B. Martin, M. B. Schaffler, and C. H. Turner, "Bone microdamage and skeletal fragility in osteoporotic and stress fractures," J. Bone Miner. Res. **12**(1), 6–15 (1997).
35. T. Buchwald, K. Niciejewski, M. Kozielski, M. Szybowicz, M. Siatkowski, and H. Krauss, "Identifying compositional and structural changes in spongy and subchondral bone from the hip joints of patients with osteoarthritis using Raman spectroscopy," J. Biomed. Opt. **17**(1), 017007 (2012).
36. M. Grant, J. Wilson, P. Rock, and I. Chapple, "Induction of cytokines, MMP9, TIMPs, RANKL and OPG during orthodontic tooth movement," Eur. J. Orthod. **35**(5), 644–651 (2013).
37. A. Dudic, S. Kiliaridis, A. Mombelli, and C. Giannopoulou, "Composition changes in gingival crevicular fluid during orthodontic tooth movement: comparisons between tension and compression sides," Eur. J. Oral Sci. **114**(5), 416–422 (2006).
38. S. A. Alfaqeeh and S. Anil, "Lactate dehydrogenase activity in gingival crevicular fluid as a marker in orthodontic tooth movement," Open Dent. J. **5**(1), 105–109 (2011).
39. V. A. Iconomidou, D. G. Chryssikos, V. Gionis, M. A. Pavlidis, A. Paipetis, and S. J. Hamodrakas, "Secondary structure of chorion proteins of the teleostean fish Dentex dentex by ATR FT-IR and FT-Raman spectroscopy," J. Struct. Biol. **132**(2), 112–122 (2000).
40. A. Torreggiani, G. Bottura, and G. Fini, "Interaction of biotin and biotinyl derivatives with avidin: conformational changes upon binding," J. Raman Spectrosc. **31**(5), 445–450 (2000).
41. A. Torreggiani and A. Tinti, "Raman spectroscopy a promising technique for investigations of metallothioneins," Metallomics **2**(4), 246–260 (2010).
42. A. M. Herrero, "Raman spectroscopy for monitoring protein structure in muscle food systems," Crit. Rev. Food Sci. Nutr. **48**(6), 512–523 (2008).
43. T. Miura and G. J. Thomas, Jr., "Raman spectroscopy of proteins and their assemblies," Subcell. Biochem. **24**, 55–99 (1995).

1. Introduction

Orthodontic tooth movement based on alveolar bone and periodontal ligament remodeling is a continual, balanced process characterized by bone deposition and resorption [1, 2]. During orthodontic treatment, periodontal tissues respond rapidly to mechanical stress, with consequent metabolic changes that allow tooth movement. The initial orthodontic tooth movement phase includes diverse inflammatory responses by periodontal tissue, and is characterized by alterations in blood flow, changes in oxygen tension, periodontal vasodilation, and leukocyte migration out of capillaries [3].

Gingival crevicular fluid (GCF) is an oral cavity-specific inflammatory exudate with constituents derived from a variety of sources, including inflammatory cells, microbial dental plaque and serum [4, 5]. GCF flow rate and composition change relative to periodontal tissue condition. GCF is released into the crevicular sulcus at a 3 μl/h flow rate under normal conditions. However, during inflammation, GCF flow rate is increased up to 443 μl/h, and GCF composition changes [6]. In recent years, GCF analysis has been proposed as a diagnostic marker for periodontal ligament and bone remodeling during orthodontic tooth movement [7–10].

To evaluate the changes in GCF near teeth subjected to orthodontic forces, conventional biological methods such as enzymatic activity with molecular specificity are widely used [9, 11–13]. However, these traditional methods are very time-consuming and labor-intensive, with complicated procedures and large amounts of material required.

Vibrational spectroscopy, such as infrared (IR) spectroscopy, has also been used to examine GCF in periodontitis [14, 15]. Recently, Liu *et al*. studied periodontitis-specific molecular signatures in GCF using IR spectroscopy [14]. They also showed diabetes-associated periodontitis GCF molecular features using IR spectroscopy. Spectral analysis revealed several molecular signatures in periodontitis diabetic subject GCF compared to non-diabetic controls [15]. They suggest IR spectroscopy is a feasible method for differentiating GCF disease-specific molecular signatures. However, IR spectroscopy has some disadvantages, such as strong interference from water, as well as a broad spectrum. In contrast, Raman spectroscopy shows minimal sensitivity to interference from water, and it has better spatial resolution than IR spectroscopy. Furthermore, because Raman bands are inherently sharper than their infrared counterparts, isolated bands are often present in the

#216711 - $15.00 USD Received 9 Jul 2014; revised 28 Aug 2014; accepted 1 Sep 2014; published 10 Sep 2014

spectrum, allowing more straightforward quantitative analysis. Raman spectroscopy has recently emerged as a powerful modality for the diagnosis of several diseases, and can be used to detect changes in analyte structure and composition at the molecular level due to being non-invasive, highly sensitive, and label-free [16–19]. In addition, it is widely accepted in the dentistry field, which diagnoses and treats human oral cavity diseases [20–23].

This longitudinal study used Raman spectroscopy to characterize GCF biochemical analytes by treatment time and tooth movement during orthodontic treatment in human subjects.

2. Materials and methods

2.1. Subjects

Ten subjects (7 females and 3 males) aged 18–26 years (mean ± SD, 20.8 ± 2.5) participated in this study. Table 1 presents inclusion criteria. Orthodontic patients were not administered any anti-inflammatory agents throughout the study period. Intensive periodontal care was used to verify healthy gingiva in all patients. This study was approved by the Kyung Hee University Dental Hospital Institutional Review Board (IRB No.: KHD IRB 1401-1).

Table 1. Inclusion criteria for patient selection.

Inclusion criteria
(1) Mild-to-moderate maxillary and mandibular arch crowding (Arch length discrepancy: 4-7 mm)
(2) Class I molar relationship
(3) Treatment modality: non-extraction
(4) Good periodontal health (probing depth not exceeding 3 mm for the whole dentition)
(5) No anti-inflammatory agents or antibiotic use prior to the study
(6) Healthy without systemic diseases or craniofacial anomalies
(7) No previous orthodontic treatment history
(8) Non-smoker

2.2. GCF collection

As a control, GCF samples were collected from target teeth prior to bonding, and 1, 7 and 28 days after orthodontic force application. Figure 1 shows GCF collection procedures. Before GCF collection, supragingival plaque was removed, and target teeth were isolated with cotton pellets, then air dried for 5 sec as previously described [12, 24]. GCF was collected with no. 30 standardized sterile paper strips (Inline; Torino, Italy) inserted 1 mm into the gingival crevice and left *in situ* for 60 sec. Three strips were used at 60-sec intervals to maximize GCF volume per site. Care was taken to avoid mechanical injury. Immediately after collection, paper points were transferred to Eppendorf tubes and stored at −80 °C.

2.3. Raman spectroscopic measurements

In order to obtain Raman spectroscopic measurements, all strips were inserted into 1.5-mL Eppendorf tubes containing 10 μl distilled water and centrifuged (10 min at 2000 rpm) to elute GCF components. Samples obviously contaminated with blood were discarded. GCF samples (5 μl) were deposited onto gold-coated substrate, then dried at room temperature. Raman spectra were acquired using a SENTERRA confocal Raman system (Bruker Optics Inc., Billerica, MA, USA) equipped with a 785-nm diode laser source (100 mW before objective) at a resolution of 3 cm^{-1}. A 100 × air objective (MPLN N. A. 0.9, Olympus), which produced a ~1 μm laser spot size, was used to collect Raman signals. GCF Raman spectra were calculated as the average of ten measurements at arbitrary sites on the dried drops. Baseline correction was performed by the rubber-band method, which was used to stretch between the spectrum endpoints. All Raman measurements were recorded with a 60-sec accumulation time in the 650-1750 cm^{-1} range, and spectral acquisitions were carried out using OPUS software.

#216711 - $15.00 USD Received 9 Jul 2014; revised 28 Aug 2014; accepted 1 Sep 2014; published 10 Sep 2014

2.4. Data analysis

Baseline corrected spectra were intensity normalized to carbonate band intensity at 1088 cm^{-1}. Raman bands in baseline corrected spectra were fitted with a Gaussian function using the Origin 8.0 program. Curve fitting results were accepted when the residuals were minimized ($R^2 > 0.99$).

Data normality was confirmed with the Shapiro-Wilk normalcy test ($P > 0.05$), and homogeneity of variance was confirmed with Levene's test ($P > 0.05$). After orthodontic force application, one-way ANOVA was used to analyze changes in mineralization index and carbonate accumulation in GCF by time. In addition band Tukey's HSD post-hoc procedure was used to assess individual measurement differences by time. Pearson correlation analysis was used to assess the relationship between mineralization index and carbonate accumulation. Data were analyzed using SPSS version 18 (Chicago, IL, USA).

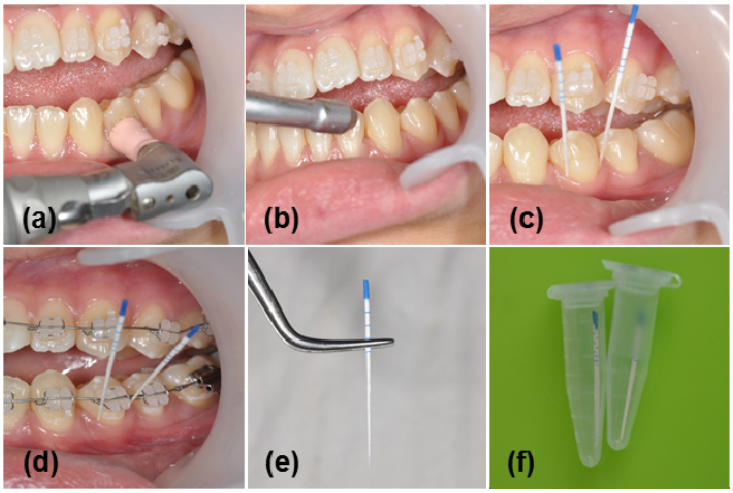

Fig. 1. Collection procedures for gingival crevicular fluid (GCF). (a) Prophylaxis, (b) drying the target area, (c) GCF collection before orthodontic force loading, (d) GCF collection after orthodontic force loading, (e) paper point with absorbed GCF, and (f) paper point in Eppendorf tubes.

3. Results and discussion

A Raman peak is uniquely defined by spectral parameters, including Raman shift, intensity, and full width at half maximum (FWHM). These features reveal information about specific molecular vibrations. Figure 2 shows the normalized average GCF Raman spectrum before orthodontic treatment. Peak assignments for GCF are given in Table 2. The Raman spectrum in Fig. 2 consists of peaks corresponding to cellular component molecular vibrations, including nucleic acids, proteins, lipids, and other metabolic compounds [25–29]. Proteins are major GCF chemical components. Glycosaminoglycans (GAGs) are a minor GCF component group. GAGs are a heterogeneous group of linear polysaccharides, each built around a relevant core protein (i.e., proteoglycans), found in connective tissue extracellular matrix [30, 31]. Although Raman bands from glycosaminoglycans (GAGs) can overlap with some protein bands, they present as relatively weak Raman scatters, and thus do not contribute significantly to overall GCF spectra. However, protein interaction with GAGs and lipids may still influence protein spectral features, such as band position, width, intensity or area.

#216711 - $15.00 USD Received 9 Jul 2014; revised 28 Aug 2014; accepted 1 Sep 2014; published 10 Sep 2014

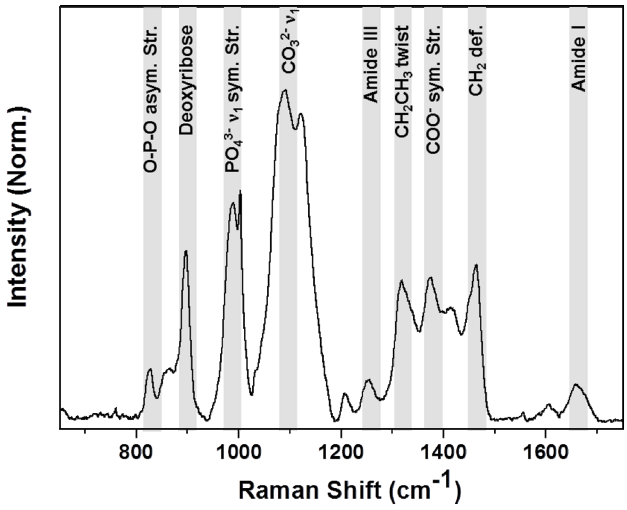

Fig. 2. Normalized average GCF Raman spectrum without orthodontic treatment

Table 2. Gingival crevicular fluid Raman spectra peak assignment [25–29].

Peak (cm-1)	Band assignment	Component
825	O-P-O asym. str.	DNA/RNA
856	Ring br. Tyr	protein
895	Deoxyribose	DNA/RNA
984	PO_4^{3-} ν_1 sym. str.	Phosphate (HA)
1002	Sym. Ring br. Phe	protein
1088	CO_3^{2-} ν_1 sym. str	carbondte apatite
1120	C-O, C-C str.	DNA/RNA, protein
1207	C-C_6H_5 str. Phe, Trp	protein
1250	Random coil, Amide III	Protein
1314	CH_2CH_3 tw.	Protein (collagen)
1372	COO^- sym. str.	HA
1411	COO^- sym. str.	HA
1463	CH_2	Lipids, protein, nucleic acid
1554	Amide II	protein
1602	Phe.	protein
1658	α-helix, Amide I	protein

[a]Abbreviations: Phe, phenylalanine; Tyr, tyrosine; Trp, tryptophan; br, breathing; str, stretching; sym, symmetric; asym, asymmetric; tw, twist.

The 825 and 895 cm^{-1} peaks represent asymmetric O-P-O stretching mode vibrations and deoxyribose in the nucleic acids, respectively. Protein Raman bands can be observed at 1002, 1250, 1314, and 1658 cm^{-1}. The sharp band at 1002 cm^{-1} corresponds to phenylalanine ring stretching. The peaks at 1250 and 1658 cm^{-1} represent amide III (random coil) and amide I (α-helix), respectively. The band at 1314 cm^{-1} is assigned to the CH_3CH_2 collagen twisting mode. The band at 1463 cm^{-1} (CH_2) can be attributed to nucleic acid, proteins and lipids. Other molecular vibrations are presented in Table 2. Mineral apatite was also observed at 984,

#216711 - $15.00 USD Received 9 Jul 2014; revised 28 Aug 2014; accepted 1 Sep 2014; published 10 Sep 2014

1088, 1372 and 1411 cm^{-1}. The band at 984 cm^{-1} was assigned to phosphate ion PO_4^{3-} symmetric stretch mode, the peaks at 1372 and 1411 cm^{-1} represent COO^- symmetric stretch, which are associated with hydroxyapatite. The strong band at 1088 cm^{-1} was assigned to carbonate ion CO_3^{2-} symmetric stretching mode, which is associated with carbonate-apatite.

Figure 3 shows GCF normalized average Raman spectra before (baseline, 0 days) and 1, 7 and 28 days after orthodontic treatment. Raman spectroscopy is widely used to evaluate alterations in bone composition associated with aging, disease, or injury [32–34]. The Raman spectrum major band assignments for bone minerals have been established, so band intensity ratios can be used as experimental measures for phosphate/amide I, carbonate/phosphate, and carbonate/amide I ratios. For phosphate, carbonate and matrix markers, we used phosphate PO_4^{3-} symmetric stretch (984 cm^{-1}), carbonate CO_3^{2-} symmetric stretch (1088 cm^{-1}) and collagen amide I (1667 cm^{-1}), which appear as gray zones in Fig. 3.

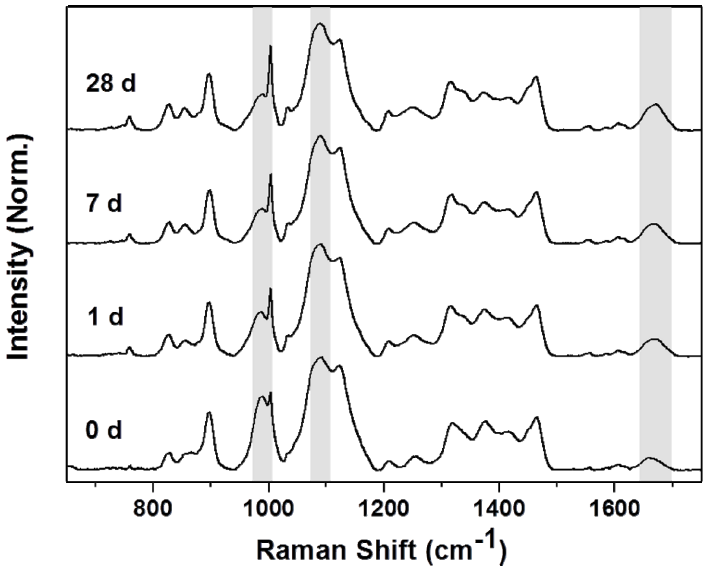

Fig. 3. Normalized average Raman spectra for control GCF (0 d) and early-phase GCF tooth movement at day 1, 7 and 28 (1 d, 7 d and 28 d).

Figure 4 presents the hydroxyapatite to primarily collagen-dominated matrix band (phosphate 984 cm^{-1}/ amide I 1667 cm^{-1}) intensity ratio, which indicates the amount of mineralization [33]. Hydroxyapatite/collagen ratios were decreased at day 7 ($P < 0.05$), indicating less mineralization due to a reduction in hydroxyapatite content during the alveolar bone remodeling process [34]. Another mineral-related parameter included carbonate-to-amide I (1088 cm^{-1}/1667 cm^{-1}) ratio, which is shown in Fig. 5. This was similar to the phosphate-to-amide I ratio, and decreased on day 7 ($P < 0.05$).

Figure 6 shows the carbonate apatite to hydroxyapatite ratio (carbonate 1088 cm^{-1}/phosphate 984 cm^{-1}) at baseline, and during orthodontic treatment at 1, 7 and 28 days. The carbonate apatite to hydroxyapatite ratio is a spectroscopic parameter which indicates carbonate ion substitution into the apatite mineral. Carbonate accumulation extent in the apatite crystal lattice was significantly higher on day 7 than day 0 ($P < 0.05$). This result indicated that the amount of carbonate accumulated in the apatite crystal lattice was increased due to deficient mineralization during the alveolar bone remodeling process [35].

#216711 - $15.00 USD Received 9 Jul 2014; revised 28 Aug 2014; accepted 1 Sep 2014; published 10 Sep 2014

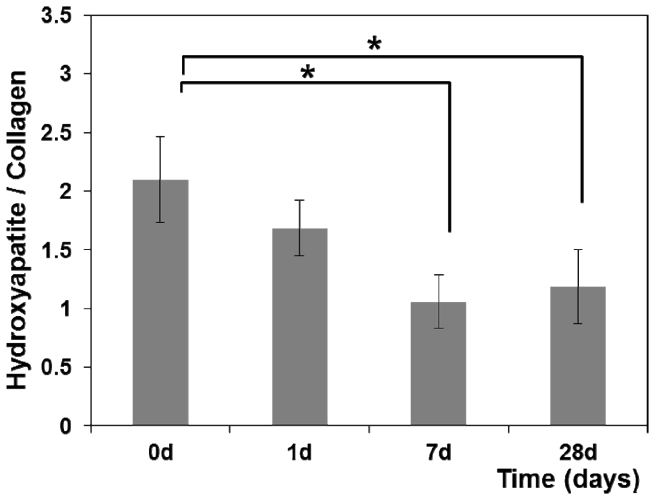

Fig. 4. Hydroxyapatite to collagen (phosphate 984 cm^{-1}/ amide I 1667 cm^{-1}) ratio in GCF during orthodontic treatment. *Significantly different from day 0 ($P < 0.05$, one-way ANOVA with Turkey's HSD post-hoc procedure)

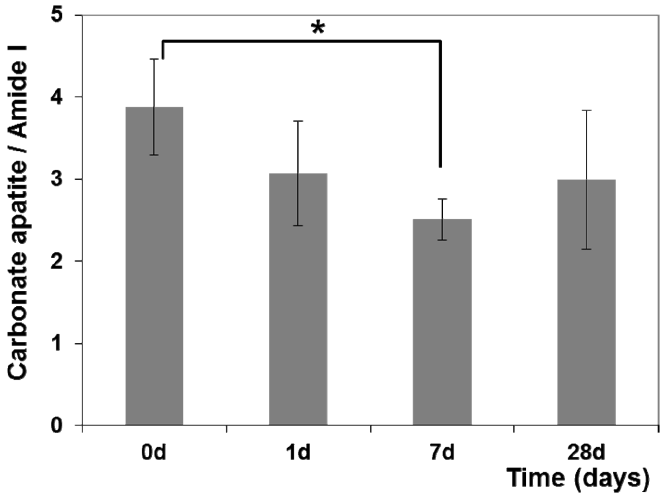

Fig. 5. Carbonate apatite to collagen (carbonate 1088 cm^{-1}/ amide I 1667 cm^{-1}) ratio in GCF during orthodontic treatment. *Significantly different from day 0 ($P < 0.05$, one-way ANOVA with Turkey's HSD post-hoc procedure)

#216711 - $15.00 USD Received 9 Jul 2014; revised 28 Aug 2014; accepted 1 Sep 2014; published 10 Sep 2014

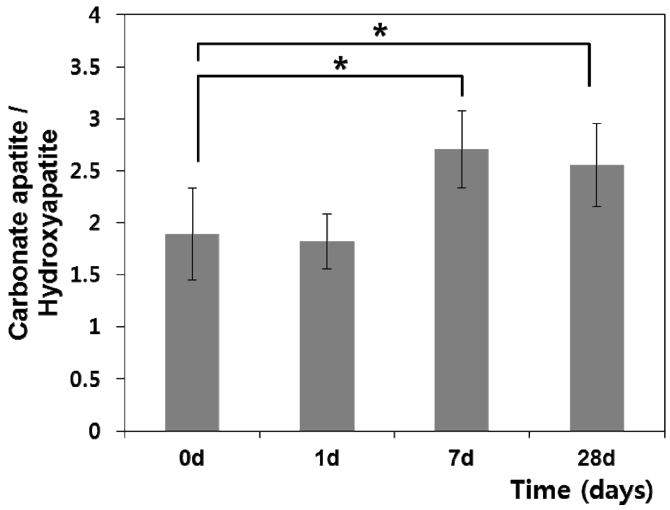

Fig. 6. Carbonate apatite to hydroxyapatite (carbonate 1088 cm^{-1}/ phosphate 984 cm^{-1}) ratio in GCF during orthodontic treatment. *Significantly different from day 0 ($P < 0.05$, one-way ANOVA with Turkey's HSD post-hoc procedure)

Pearson correlation analysis revealed a significant negative correlation between the hydroxyapatite to collagen and carbonate apatite to hydroxyapatite ratios ($r = –0.697$, $P < 0.001$) (Table 3). A high carbonate/phosphate ratio was associated with a low phosphate/amide I ratio. This is in good agreement with previous evidence [33–35].

Table 3. Correlation between hydroxyapatite to collagen peak intensity ratio and carbonate apatite to hydroxyapatite peak intensity ratio.

		Carbonate apatite/hydroxyapatite (1088 cm^{-1}/984 cm^{-1})
Hydroxyapatite/collagen (984 cm^{-1}/1667 cm^{-1})	Pearson coefficient	-0.697
	P value	0.001**

*Pearson correlation analysis. ** P<0.001*

GCF Raman spectral analysis assessed bone mineralization and carbonate accumulation degree in the apatite crystal lattice. Peak levels were seen on day 7 following retraction initiation. As alveolar bone remodeling increased, mineral/matrix ratios decreased, and carbonate apatite/hydroxyapatite ratios increased. Therefore, these band intensity ratios (carbonate apatite/hydroxyapatite and hydroxyapatite/collagen) could be used as GCF Raman markers during orthodontic tooth movement.

GCF is an exudate derived from a variety of sources, and contains proteins such as cytokines, enzymes, and metabolites. Protein amount in this fluid increased with inflammation and capillary permeability, and biochemical change occurred during orthodontic force application. Amide I is a basic protein structural component that is extremely sensitive to structural changes. Thus we analyzed the Raman spectra in more detail in the amide I (1625–1715 cm^{-1}) range.

Figure 7(A) shows Raman peak 1667 cm^{-1} relative intensity at baseline, and during orthodontic treatment at 1, 7 and 28 days. Raman spectra exhibited significant time dependence; Raman peak intensity increased at day 7 and decreased by day 28. This suggests an increase in the presence or a change in the conformation of proteins at day 7. Intensity reduction at day 28 may be due to decreased orthodontic wire force. Previous studies have

#216711 - $15.00 USD Received 9 Jul 2014; revised 28 Aug 2014; accepted 1 Sep 2014; published 10 Sep 2014

analyzed cytokines, enzymes, and metabolites found in GCF during orthodontic tooth movement [12, 36–38]. Dudic *et al*. studied GCF composition changes during the early phase of orthodontic tooth movement (1 min, 1 h, 1 day, and 7 days) [37]. They showed that interleukin-1β (IL-1 β), substance P (SP), and prostaglandin E_2 (PGE_2) GCF levels near orthodontically moved teeth were significantly higher than those near control teeth for both tension and compression sides. Anil *et al*. reported GCF lactate dehydrogenase (LDH) activity was significantly higher on day 7, 14, and 21 where orthodontic force was applied [38].

This experiment showed notable peak shifts during orthodontic tooth movement [Fig. 7(B)]. The 1658 cm^{-1} (amide I, α-helix) peak at baseline was red-shifted to 1667 cm^{-1} at day 1 and 7, and 1671 cm^{-1} at day 28 during orthodontic treatment. Bands at 1667 and 1671 cm^{-1} were assigned to the amide I β-sheet. These peak shifts might be used as Raman markers for orthodontic tooth movement chemical changes.

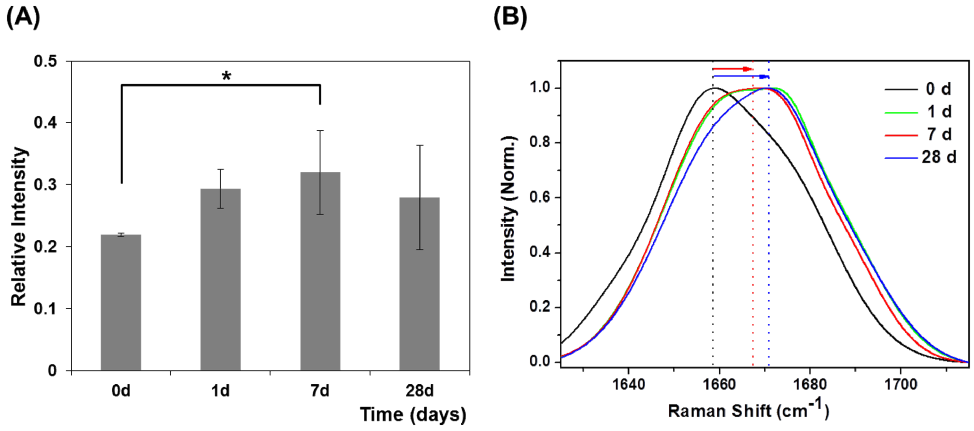

Fig. 7. (A) Relative intensities in 1667 cm^{-1} Raman peaks during orthodontic treatment. *Significantly different from day 0 ($P < 0.05$, one-way ANOVA with Turkey's HSD post-hoc procedure). (B) Normalized average GCF Raman spectra in the 1625-1715 cm^{-1} range during orthodontic treatment.

As shown in Fig. 7(B), there was a broad spectrum in the amide I range. There are a multitude of single bands at different wavenumbers, which can be resolved into multiple components attributable to different secondary structures (Table 3) [39–41]. Thus, we performed curve fitting in the amide I range to show contributions from different secondary conformations.

Figure 8 shows the experimental data: fitted peaks and the summation of fitting curves for GCF characteristic spectra in the 1625-1715 cm^{-1} range at baseline (0 day), and day 1, 7 and 28 during orthodontic treatment. The center peak, relative area and bandwidth are shown in Table 4. Three Raman spectral components were seen in the 1625-1715 cm^{-1} region. These spectra showed significant differences at baseline and day 1, 7 and 28 during orthodontic treatment, reflecting differences in protein secondary structure. The amide I peak fit without orthodontic treatment showed major intensity in the component band at 1671 cm^{-1} (β-sheet), with a relative area of 59.2% and FWHM of 26.4 cm^{-1}. Component bands at 1638 cm^{-1} (12.8%) and 1655 cm^{-1} (28.0%) made a minor contribution. Bands at 1638 and 1655 cm^{-1} were markers for β-turn and α-helical peptide bonds, respectively [42, 43]. During orthodontic treatment at day 1, 7 and 28, GCF exhibited triple bands in similar positions to each other. However, there was little difference in relative area and width. During orthodontic treatment at day 7, the major amide I band feature was centered at 1661 cm^{-1} (random coil), with a relative area of 75.8%, and FWHM of 27.3 cm^{-1}, indicating a random coil structure predominance. The component band near 1674 cm^{-1} (5.9%) suggested a minor β-sheet

#216711 - $15.00 USD Received 9 Jul 2014; revised 28 Aug 2014; accepted 1 Sep 2014; published 10 Sep 2014

contribution in GCF during orthodontic treatment (Table 5). This demonstrated that random coil conformation increased and β-sheet structure decreased during orthodontic tooth movement, indicating either GCF protein structural rearrangement, or expression of a new set of proteins with different structural characteristics.

Therefore, curve fitting analyses demonstrated that Raman spectroscopy is able to characterize secondary structure ensembles. Furthermore, Raman spectra changes associated with protein secondary structures can be used as markers for GCF chemical changes during orthodontic tooth movement.

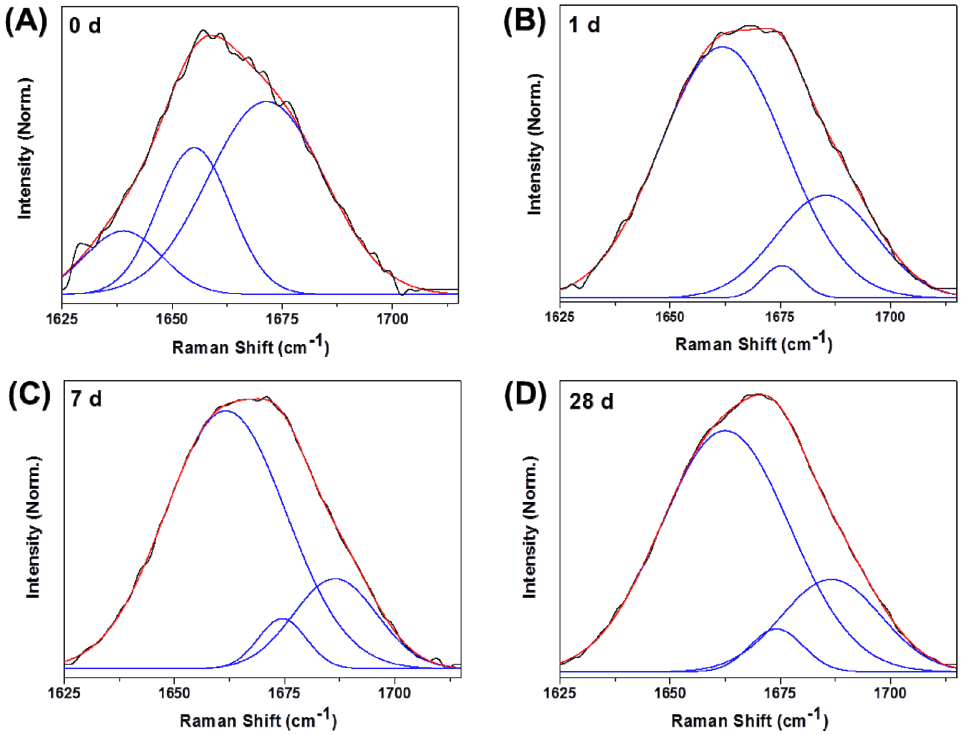

Fig. 8. Normalized average GCF Raman spectra curve-fitting during orthodontic tooth movement (0, 1, 7 and 28 days) in the 1625-1715 cm^{-1} range. The black lines represent experimental data. The blue and red lines illustrate fitted peaks and summation of fitting curves, respectively.

Table 4. Principal Raman band wavenumbers characteristic of secondary protein structure in the amide I range [39–41].

Conformation	Raman bands (cm^{-1})
α-helix	1650-1657
β-sheet	1668-1675
β-turn	1639-1649, 1673-1700
Random/disorder	1660-1665

#216711 - $15.00 USD Received 9 Jul 2014; revised 28 Aug 2014; accepted 1 Sep 2014; published 10 Sep 2014

Table 5. Curve fitting averaged Raman spectra in the 1625–1715 cm^{-1} range.

day	peak no.	center (cm^{-1})	relative area (%)	width (cm^{-1})
	1	1638	12.8	17.4
0	2	1655	28.0	16.4
	3	1671	59.2	26.4
	1	1662	73.2	28.3
1	2	1675	2.9	8.6
	3	1685	23.9	22.6
	1	1661	75.8	27.3
7	2	1674	5.9	10.9
	3	1686	18.3	18.9
	1	1662	73.0	29.2
28	2	1674	5.4	12.1
	3	1686	21.6	22.5

In this study, we evaluated, for the first time, Raman spectroscopy for the characterization of biochemical changes during the early phase of orthodontic tooth movement. The results from Raman spectroscopy of GCF have great potential for providing the changes at the target tooth site over time and response of periodontal tissues to orthodontic tooth movement. If orthodontic force for tooth movement is too strong or weak, the parameters such as mineral-to-matrix and carbonate apatite-to-hydroxyapatite band intensity ratios may be altered because of different response in periodontal tissue. By analyzing these parameters, the proper orthodontic force could be estimated. Furthermore, recently, the many appliances such as photobiomodulator have been developed to accelerate a tooth movement. However, the biological evidence of these devices is much insufficiency, yet. For the applying to photobiomodulator, GCF Raman spectral analysis could give to us information of mineralization degree related to alveolar bone remodeling. This technology could be used to estimate the effect of tooth movement acceleration appliance. In future study, we will investigate the effect of the photobiomodulation during orthodontic tooth movement using the GCF Raman spectroscopy. Raman spectroscopy could be used diagnostic and prognostic tool for monitoring orthodontic tooth movement in a clinical setting.

4. Conclusion

In summary, we applied Raman spectroscopy to monitor human GCF biochemical responses during early orthodontic tooth movement. Raman spectra GCF analysis showed bone mineralization degree and carbonate accumulation in the apatite crystal lattice. Peak levels were seen on day 7 following retraction initiations. As alveolar bone remodeling increased, mineral/matrix ratios decreased, and carbonate apatite/hydroxyapatite ratios increased. This might be due to deficient mineralization in the alveolar bone remodeling process.

Parameters such as mineral-to-matrix and carbonate apatite-to-hydroxyapatite band intensity ratios, and protein secondary structure curve fitting in the amide I region indicated alternations in GCF composition and structure during orthodontic tooth movement. These parameters could be used as GCF Raman markers during orthodontic tooth movement. Therefore, Raman spectroscopy may be a suitable candidate for evaluating GCF change during orthodontic tooth movement.

#216711 - $15.00 USD Received 9 Jul 2014; revised 28 Aug 2014; accepted 1 Sep 2014; published 10 Sep 2014

Acknowledgment

This work was supported by a grant from Kyung Hee University in 2013 (KHU-20131081).

#216711 - $15.00 USD Received 9 Jul 2014; revised 28 Aug 2014; accepted 1 Sep 2014; published 10 Sep 2014